

Investigation of localization effect in GaN-rich InGaN alloys and modified band-tail model

CHUAN-ZHEN ZHAO^{1,*}, BIN LIU², DE-YI FU², HUI CHEN², MING LI², XIANG-QIAN XIU², ZI-LI XIE², SHU-LIN GU² and YOU-DOU ZHENG²

¹School of Electronics and Information Engineering, Tianjin Polytechnics University, Tianjin 300160, China

²Jiangsu Provincial Key Laboratory of Advanced Photonic and Electronic Materials, Nanjing National Laboratory of Microstructures, Department of Physics, Nanjing University, Nanjing 210093, China

MS received 28 April 2011; revised 25 September 2012

Abstract. The temperature-dependent PL properties of GaN-rich $\text{In}_x\text{Ga}_{1-x}\text{N}$ alloys is investigated and S-shaped temperature dependence is observed in all InGaN samples. It is found that the origin of localization effect in samples A and B are different from that in sample C. For samples A and B, In content fluctuations should be the origin of localization effect, while the localization effect can be attributed to In-rich clusters and metallic indium inclusions for sample C. In addition, the band-tail model is modified and the modified band-tail model is used to investigate the degree of localization effect in the three samples.

Keywords. InGaN; localization effect; temperature dependence; modified band-tail model.

1. Introduction

The III nitrides and their alloys have been extensively studied due to their potential applications in optoelectronic devices. In particular, $\text{In}_x\text{Ga}_{1-x}\text{N}$ alloys are very promising, because they have a tunable direct bandgap varying from 0.7 to 3.42 eV, which makes $\text{In}_x\text{Ga}_{1-x}\text{N}$ alloy a key material in fabricating GaN-based blue light emitting diodes (LEDs) and laser diodes (LDs). So far, temperature-dependent optical properties of $\text{In}_x\text{Ga}_{1-x}\text{N}$ alloys have been investigated by several groups (Shan *et al* 1995, 1996, 1998; Smith *et al* 1996; Eliseev *et al* 1997; Narukawa *et al* 1997; Cho *et al* 1998; Schenk *et al* 2000; Wang *et al* 2000; Li *et al* 2001; Cao *et al* 2003; Chung *et al* 2003; Ramaiah *et al* 2004; Wang *et al* 2004; Yu *et al* 2004; Cheng *et al* 2005; Kazlauskas *et al* 2005; Na *et al* 2006; Usov *et al* 2007; Chang *et al* 2009; Zhao *et al* 2012a). However, very few systematic investigations on temperature-dependent photoluminescence (PL) properties of GaN-rich $\text{In}_x\text{Ga}_{1-x}\text{N}$ alloys have been reported. We have analysed the photoluminescence (PL) properties depending on temperature as well as composition in literature (Zhao *et al* 2012a), but the analysis is not deep enough. In this paper, we further investigate temperature-dependent PL properties of GaN-rich $\text{In}_x\text{Ga}_{1-x}\text{N}$ alloys and try to understand the origin of localization effect in Ga-rich InGaN alloys. In addition, the band-tail model is modified and this is used to investigate the degree of localization effect in three samples.

2. Experimental

$\text{In}_x\text{Ga}_{1-x}\text{N}$ epilayers were grown on *c*-plane GaN/sapphire substrates by metal-organic chemical vapour deposition (MOCVD). After the growth of 2 μm -thick undoped GaN layer on sapphire substrates at 1050 °C, 60 nm thick GaN buffer layer was grown at 570 °C. For InGaN growth, details have been reported in literature (Zhao *et al* 2012a). The samples were characterized by PL spectra, X-ray diffraction (XRD) and atomic force microscopy (AFM). PL spectra from 10 to 300 K were measured using 325 nm line of 20 mW He–Cd laser as excitation. XRD measurements for the three samples have been reported in the literature (Zhao *et al* 2012a). Based on XRD measurements and PL spectra, In content for samples A, B and C could be estimated to be 0.10, 0.15 and 0.25, respectively.

3. Results and discussion

Figure 1 shows PL spectra of three samples at 20 K. It is observed that the PL spectral peak positions redshift with increasing In content, x . The line shape of the PL emissions in the samples is asymmetric with a long low energy tail and a sharp high energy cut-off. The characteristic PL line shape is typical for the recombination of excitons trapped by the potential fluctuation at the band edge. We can also observe that the line shape of the PL emission for sample C is more asymmetric than those for samples A and B, which implies that the degree of localization effect in sample C is stronger than that in samples A and B.

*Author for correspondence (as3262001@yahoo.com.cn)

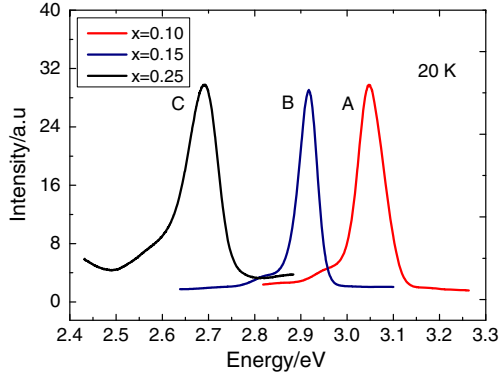


Figure 1. PL spectra of three $\text{In}_x\text{Ga}_{1-x}\text{N}$ samples at 20 K.

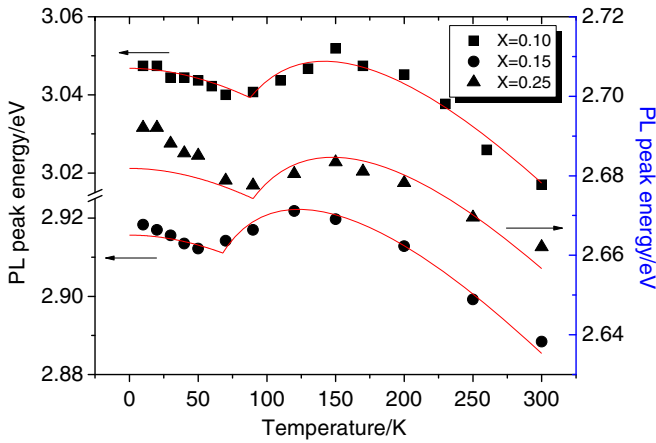


Figure 2. Temperature dependence of PL peak energies for samples (Zhao *et al* 2012a). Solid lines are fitting curves using modified band-tail model.

The temperature-dependent PL spectral peak positions for three $\text{In}_x\text{Ga}_{1-x}\text{N}$ samples are plotted in figure 2 (Zhao *et al* 2012a). It can be seen that S -shaped trend (i.e. a red-blue-redshift with increasing temperature) is observed in the whole temperature range for all the three samples. The S -shaped dependence has also been observed in AlGaIn (Bell *et al* 2004). For InGaIn alloys, the calculated phase diagrams indicate a significant phase miscibility gap (Ho and Stringfellow 1996; Saito and Arakawa 1999; Ferhat and Bechstedt 2002; Caetano *et al* 2006; Liu and Zunger 2008), so clustering and phase separation are normally found. Clustering and phase separation can lead to compositional inhomogeneity, and this can cause potential fluctuation. Under this condition, excitons in different parts should experience the fluctuated potential. When $k_B T$ is large enough, excitons have sufficient thermal energy to overcome the potential barriers and relax down to the lowest potential minima. In this temperature region, exciton localization effect is not obvious. The main factor influencing E_{peak} is the band shrink effect, so E_{peak} increases with decrease of temperature in the high temperature region. Exciton localization effect is gradually obvious with the decrease of temperature. At some tempe-

rate, localization effect influencing E_{peak} is larger than the band shrink effect, so that E_{peak} decreases with decreasing temperature. When temperature is low enough, $k_B T$ is insufficient for excitons to overcome the potential barriers. The excitons can be frozen out in the local minima and no further relaxation is possible. Under this condition, localization effect reaches saturation. If temperature goes on decreasing after saturation, E_{peak} can increase due to the band shrink effect.

Two extremums can be seen for each S -shaped temperature dependence. One is the minimum of E_{peak} and the other is the maximum of E_{peak} . The minimum of E_{peak} between redshift and blueshift regions corresponds to a temperature (hereafter $T_{\text{redshift-blueshift}}$). $T_{\text{redshift-blueshift}}$ is a temperature at which the localization effect reaches saturation. If the effective potential fluctuation is very large, the excitation can be confined in the local potential minima even if the temperature is not very low. The maximum of E_{peak} between the blueshift and redshift regions also corresponds to a temperature (hereafter $T_{\text{blueshift-redshift}}$). $T_{\text{blueshift-redshift}}$ is a temperature at which the localization effect starts to be observed obviously with decreasing temperature. The stronger the localization effect is, broader the temperature region that the localization effect influences. If the localization effect is strong enough, its effect on E_{peak} is still obvious at a relatively high temperature. Considering the above reasons, $T_{\text{redshift-blueshift}}$ and $T_{\text{blueshift-redshift}}$ can be considered as parameters to estimate the effective potential fluctuation qualitatively. The experimental results about AlGaIn alloys support this opinion (Bell *et al* 2004). From figure 2, it is found that the degree of effective potential fluctuation in the three samples are sample C > sample A > sample B. In addition, we observe that the extent of dip in the S -shape curves of the three samples are different. Similar phenomena have been reported in the literature (Cheng *et al* 2005). It is obvious that the dip in the S -shape curve of sample C is clearer than those of samples A and B, which implies that the carrier localization in sample C is stronger than that in samples A and B.

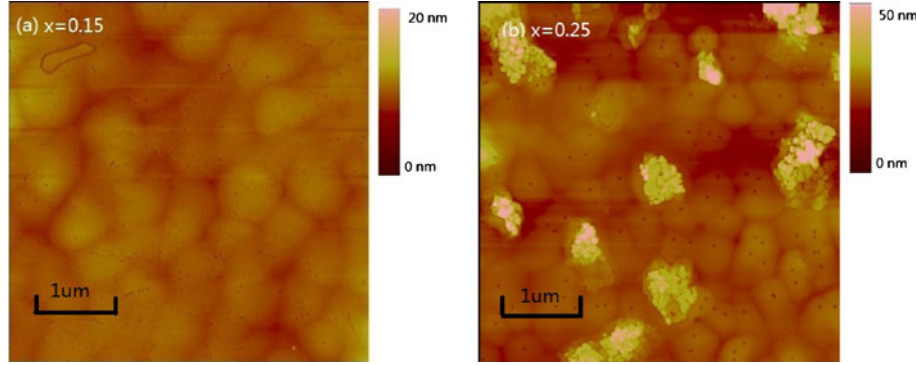
The band-tail model is usually used to investigate the degree of localization effect. In the band-tail model, the emission energy depending on the temperature could be given by the following expression (Eliseev *et al* 1997).

$$E_{\text{peak}}(T) = E_{g(0)} - \frac{\gamma T^2}{T + \theta} - \frac{\sigma^2}{k_B T}, \quad (1)$$

where $E_{g(0)}$ is the bandgap energy at 0 K, T the temperature in Kelvin, γ and θ are Varshni's fitting parameters. σ indicates the degree of localization effect and k_B the Boltzmann's constant. From the above form, we can see that the band-tail model can not be used in the whole temperature range, especially at low temperature. This is because the last term, $\sigma^2/k_B T$, can lead to the bandgap energy decreasing sharply while our experiments show that E_{peak} increases with decreasing temperature in the low temperature range. We consider that when the temperature is low enough, the

Table 1. Parameters used and obtained in modified band-tail model.

In content, x	$E(0)$ (eV)	γ (meV/K)	θ (K)	σ (meV)	T_0 (K)
0	–	0.68	600 (Tsen <i>et al</i> 2005)	–	–
0.1	3.099	0.653	585.4	20	88
0.15	2.961	0.640	578.1	16	68
0.27	2.737	0.614	563.5	21	90
1.0	–	0.414	454 (Wu <i>et al</i> 2003)	–	–

**Figure 3.** AFM measurements for samples B and C.

excitons can be frozen out in the local minima and no further relaxation is possible. Under this condition, the localization effect reaches saturation. After saturation, the localization effect can no longer make E_{peak} to decrease even if the temperature goes on decreasing. Considering the above factors, we introduce the frozen-out temperature for excitons in the band-tail model and modify the band-tail model in the following form

$$E_{\text{peak}}(T) = E_{g(0)} - \frac{\gamma T^2}{T + \theta} - \frac{\sigma^2}{k_B T} \quad (T > T_0), \quad (2)$$

$$E_{\text{peak}}(T) = E_{g(0)} - \frac{\gamma T^2}{T + \theta} - \frac{\sigma^2}{k_B T_0} \quad (T \leq T_0), \quad (3)$$

where T_0 is the frozen-out temperature for exciton. γ and θ parameters for InGaN are obtained by interpolation in accordance with Vegard's law. We use (2) to fit the experimental data. The values of σ for the three samples obtained by the modified band-tail model are listed in table 1. Based on the values of σ for the three samples, we can conclude that the degree of localization effects and the effective potential fluctuation in sample C is larger than those in samples A and B.

We used (3) and the parameters in table 1 to obtain the results in the low temperature range. Figure 2 shows the results. It can be seen that the modified model agrees well with the experiment for samples A and B. However, for sample C, the redshift of E_{peak} in the low temperature is a little larger than the result obtained by our model, which implies that there may be other factors influencing on E_{peak} .

Faster redshift of E_{peak} in the low-temperature region was also observed in a self-organized InAs/GaAs quantum-dot ensemble with a large size distribution (Xu *et al* 2001). We consider that as the redshift in the low-temperature region for sample C is very similar to that for the InAs/GaAs quantum-dot systems, In-rich clusters or quantum dot-like structure should exist in sample C. In order to prove this opinion and investigate the origin of localization effect, we analyse XRD measurement for the three samples reported in the literature (Zhao *et al* 2012a). For samples A and B, no In-rich clusters are obviously found, which shows that the potential fluctuation is only due to small In content fluctuation, so the origin of localization effect is due to In content fluctuation in samples A and B. For sample C, the diffraction peaks in the small angle range show that In-rich clusters exist in sample C, so it can be concluded that In-rich clusters should be an origin of localization effect.

In order to further investigate the origin of localization effect, AFM measurements for the three samples are done. As the result of AFM measurement for sample A is very similar to that for sample B, only the results of AFM measurements for samples B and C are given. Figure 3 shows AFM measurements for samples B and C. It can be seen that for sample B, no phase separation is found, which shows that small In content fluctuations should be the only origin of localization effect. For sample C, obvious metallic indium segregation is found. Based on XRD and AFM measurements, we consider that In-rich clusters and metallic indium inclusions should be the origins of localization effect in sample C. As In-rich clusters and metallic indium inclusions can cause larger potential fluctuation than small In content

fluctuation, it is easy to understand the localization effect in sample C is larger than that for samples A and B.

Based on the above analysis, we note that the origin of localized effect in samples A and B are different from that in sample C. This can be explained as follows. At 1073 K, the equilibrium solubility of InN in GaN is 6%. If the In composition lies between the spinodal limit and the miscibility gap (6–22% at 1073 K), InGaN alloys are metastable. When In content lies in the miscibility gap (>22%), phase separation are normally found in InGaN alloys. For samples A and B, the alloy composition lies between the spinodal limit and the miscibility gap. Although no phase separation is observed, they are metastable. For sample C, the composition lies in the miscibility gap and the phase separation is indeed observed. Considering the above mentioned factors, it is easy to understand the origin of localized effect in samples A and B are different from that in sample C. We also note that the origin of localized effect in degenerate InN is different from that in InGaN alloys. In degenerate InN, the origin of the localized states can be attributed to the metallic indium inclusions (Intartaglia et al 2005).

In addition, it is found that the origin of localization effect and the function of In-rich clusters in InGaN are different from those in InGaNAs. In InGaN, In-rich clusters should be an origin of localization effect. For InGaNAs, it is reported that localization effect is relative to the N content (Zhao et al 2007). The incorporation of a small amount of nitrogen can lead to a strong local potential and distortion of the crystal lattice due to the large mismatch in size and electronegativity. The more the N content is, the stronger the localization effect is. After annealing, the localization effect becomes weak or can be eliminated due to the formation of more In-rich clusters (Zhao et al 2007). It can be concluded that In-rich clusters should not be the origin of localization effect in InGaNAs. Even if In-rich clusters can cause localization effect in InGaNAs, its influence on excitons is smaller than that of N content in InGaNAs. From the above analysis, we can see that the effect of In-rich clusters in InGaN and InGaNAs are different. This is due to the different environments around In-rich clusters. In InGaN alloys, In-rich clusters are surrounded by InGaN with low In content (Zhao et al 2012b), while In-rich clusters are surrounded by InGaAs in InGaNAs alloys. Because of the different potentials around In-rich clusters, the function of In-rich clusters in InGaN and InGaNAs is very different.

4. Conclusions

In conclusion, the S-shaped temperature dependence is observed in all GaN-rich $\text{In}_x\text{Ga}_{1-x}\text{N}$ samples. It is found that the origin of localization effect in samples A and B are different from that in sample C. This can be explained by phase diagrams. In addition, the degree of localization effect in the three samples are investigated using the modified band-tail model.

Acknowledgement

This work is supported by the National Natural Science Foundation of China (60906025).

References

- Bell A et al 2004 *J. Appl. Phys.* **95** 4670
 Caetano C, Teles L K and Marques M 2006 *Phys. Rev.* **B74** 045215
 Cao X A, LeBoeuf S F, Rowland L B, Yan C H and Liu H 2003 *Appl. Phys. Lett.* **82** 3614
 Chang H S, Hsu T M, Chuang T F, Chen W Y, Gwo S and Shen C H 2009 *Solid State Commun.* **149** 18
 Cheng Y C, Wu C M, Yanga C C, Li G A, Rosenauer A, Ma K J, Shi S C and Chen L C 2005 *J. Appl. Phys.* **98** 014317
 Cho Y H, Gainer G H, Fischer A J, Song J J, Keller S, Mishra U K and DenBaars S P 1998 *Appl. Phys. Lett.* **73** 1370
 Chung Y Y et al 2003 *J. Appl. Phys.* **93** 9693
 Eliseev P G, Perlin P, Lee J and Osinski M 1997 *Appl. Phys. Lett.* **71** 569
 Ferhat M and Bechstedt F 2002 *Phys. Rev.* **B65** 075213
 Ho I and Stringfellow G B 1996 *Appl. Phys. Lett.* **69** 2701
 Intartaglia R, Maleyre B, Ruffenach S, Briot O, Taliercio T and Gil B 2005 *Appl. Phys. Lett.* **86** 142104
 Kazlauskas K, Tamulatis G, Pobedinskas P, Žukauskas A, Huang C F, Cheng Y C, Wang H C and Yang C C 2005 *Phys. Status Solidi (c)* **2** 2809
 Li Q, Xu S J, Cheng W C, Xie M H, Tong S Y, Che C M and Yang H 2001 *Appl. Phys. Lett.* **79** 1810
 Liu J Z and Zunger A 2008 *Phys. Rev.* **B77** 205201
 Na J H et al 2006 *Appl. Phys. Lett.* **89** 253120
 Narukawa Y, Kawakami Y, Funato M, Fujita S and Nakamura S 1997 *Appl. Phys. Lett.* **70** 981
 Ramaiah K S, Su Y K, Chang S J, Chen C H and Juang F S 2004 *Appl. Phys. Lett.* **85** 401
 Saito T and Arakawa Y 1999 *Phys. Rev.* **B60** 1701
 Schenk H P D, Leroux M and de Mierry P 2000 *J. Appl. Phys.* **88** 1525
 Shan W, Schmidt T J, Yang X H, Hwang S J, Song J J and Goldenberg B 1995 *Appl. Phys. Lett.* **66** 985
 Shan W, Little B D, Song J J, Feng Z C, Schurman M and Stall R A 1996 *Appl. Phys. Lett.* **69** 3315
 Shan W et al 1998 *J. Appl. Phys.* **84** 4452
 Smith M, Chen G D, Lin J Y, Jiang H X, Asif Khan M and Chen Q 1996 *Appl. Phys. Lett.* **69** 2837
 Tsen K T et al 2005 *Superlatt. Microstruct.* **38** 77
 Usov S O et al 2007 *Semicond. Sci. Technol.* **22** 528
 Wang T, Saeki H, Bai J, Shirahama T, Lachab M and Sakai S 2000 *Appl. Phys. Lett.* **76** 1737
 Wang H C, Lin S C, Lu Y C, Cheng Y C, Yang C C and Ma K J 2004 *Appl. Phys. Lett.* **85** 1371
 Wu J et al 2003 *J. Appl. Phys.* **94** 4457
 Xu Z Y et al 2001 *Phys. Rev.* **B54** 11528
 Yu H B, Chen H, Li D S and Zhou J M 2004 *Chin. Phys. Lett.* **21** 1323
 Zhao Q X, Willander M, Wang S M, Wei Y Q, Gu Q F, Sadeghi M and Larsson A 2007 *Thin Solid Films* **515** 4423
 Zhao C Z et al 2012a *Sci. China-Phys. Mech. Astron.* **55** 396
 Zhao C Z et al 2012b *Sci. China-Phys. Mech. Astron.* **55** 798